Geomechanics and Engineering, *Vol. 13, No. 6 (2017) 907-928*
DOI: https://doi.org/10.12989/gae.2017.13.6.907

Influences of seepage force and out-of-plane stress on cavity contracting and tunnel opening

Jin-Feng Zou[1a], Kai-Fu Chen[1] and Qiu-Jing Pan[*2]

[1]*School of Civil Engineering, Central South University, Hunan 410075, China*
[2]*Laboratory 3SR, Grenoble Alpes Unviersity, CNRS UMR 5521, Grenoble, France*

(Received October 16, 2016, Revised April 24, 2017, Accepted May 18, 2017)

Abstract. The effects of seepage force and out-of-plane stress on cavity contracting and tunnel opening was investigated in this study. The generalized Hoek-Brown (H-B) failure criterion and non-associated flow rule were adopted. Because of the complex solution of pore pressure in an arbitrary direction, only the pore pressure through the radial direction was assumed in this paper. In order to investigate the effect of out-of-plane stress and seepage force on the cavity contraction and circular tunnel opening, three cases of the out-of-plane stress being the minor, intermediate, or major principal stress are assumed separately. A method of plane strain problem is adopted to obtain the stress and strain for cavity contracting and circular tunnel opening for three cases, respectively, that incorporated the effects of seepage force. The proposed solutions were validated by the published results and the correction is verified. Several cases were analyzed, and parameter studies were conducted to highlight the effects of seepage force, H-B constants, and out-of-plane stress on stress, displacement, and plastic radius with the numerical method. The proposed method may be used to address the complex problems of cavity contraction and tunnel opening in rock mass.

Keywords: seepage force; out-of-plane stress; cavity contraction; generalized Hoek-Brown failure criterion

1. Introduction

A large number of elastic-plastic closed-form solutions for the problem of cavity contraction and tunnel opening exist in the literatures (Banerjee *et al.* 2016, Bousbia and Messast 2015, Carranza-Torres and Fairhurst 1999, Di *et al.* 2016, Fahimifar and Zareifard 2009, Fahimifar *et al.* 2015, Huang *et al.* 2016, Lee and Pietruszczak 2008, Liang *et al.* 2017, Lukic *et al.* 2014, Pan and Dias 2016, Shi *et al.* 2016, Yang *et al.* 2014, 2015, 2016, Zhang *et al.* 2016, Yu 2000, Shin *et al.* 2011, Wang *et al.* 2012, Zhou *et al.* 2014, 2015 and 2016, Zou and Zuo 2017, Zou *et al.* 2016, 2017c, 2017d, Zou and Du 2017, Zou and Xia 2017a, b). Some literatures also investigate characteristic behavior of granular materials or rock mass (Mohammadi *et al.* 2017, Wan *et al.* 2017, Zhuang *et al.* 2017). However, in the majority of these plane-strain solutions, the out-of-plane stress (s_z) in the plastic zone is usually assumed to be the intermediate principal stress. However, it has been shown that s_z may not remain the intermediate principal stress in the failure

*Corresponding author, Ph.D., E-mail: qiujing.pan@3sr-grenoble.fr
[a]Professor, E-mail: zoujinfeng_csu@163.com

http://www.techno-press.org/?journal=gae&subpage=7 ISSN: 2005-307X (Print), 2092-6219 (Online)

zone around the tunnel in particular, when the brittle plastic or strain softening behavior of a rock mass is taken into account. Reed (1986, 1987) indicated that, in the elastic region, it is readily seen that $s_z=q$ throughout, and thus remains the intermediate stress. In the plastic region, $s_q=s_z$ at the tunnel wall. If the tunnel support pressure is reduced below the critical value, an inner plastic zone will develop in which $s_q<s_z$. Pan and Brown (1996) indicated that the axial stress is dependent on the rock-mass dilation proposed the quasi-plane strain-softening problem of circular tunnel considering effect of out-of-plane stress. Wang *et al.* (2012) pointed out that the residual region is close to the tunnel wall with $s_q=s_z>s_r$. The softening region is divided into the inner plastic region with $s_q=s_z>s_r$ and the outer plastic region with $s_q>s_z>s_r$.

However, the effects of seepage force and out-of-plane stress on stress and displacement during cavity contracting and tunnel opening have yet to be defined clearly. For example, Mohamed (2003) proposed an exact solution of gravity flow generated in a circular tunnel, but the effects of seepage force and out-of-pane stress on stress and displacement were excluded. Lee *et al.* (2006) examined the tunnel face stability with steel pipe-reinforced multi-step grouting in underwater tunnels and determined that after the steel pipe-reinforced multi-step grouting was adopted, the seepage force decreased significantly in an underwater tunnel. The effective stresses that act on the tunnel face were determined based on the upper-bound solution and seepage pressure was calculated through seepage analysis (2001). Fahimifar and Zareifard (2009) proposed an analytical solution to analyze tunnels below the groundwater table in plane strain axisymmetric condition that considers mechanical–hydraulic coupling. However, the issue of spherical cavity contraction was not considered. Shin *et al.* (2011) investigated the interaction between tunnel supports and ground convergence by considering the seepage forces through analytical and numerical analyses. In applying the existing two-dimensional solutions to the axisymmetric tunnel problem, a number of key questions still remain unresolved. This include:

What is the influence of axial stress s_z on tunnel stability and convergence incorporating seepage force?

The present study focuses mainly on the effects of the seepage force and out-of-pane stress on the cavity contracting and tunnel opening in a generalized Hoek-Brown rock mass. The Solutions of stress and displacement were presented for the spherical and cylindrical cavities that contracted the tunnel opening. Parameter studies were performed to highlight the effects of seepage force, H–B constants, and out-of-plane stress with the numerical method.

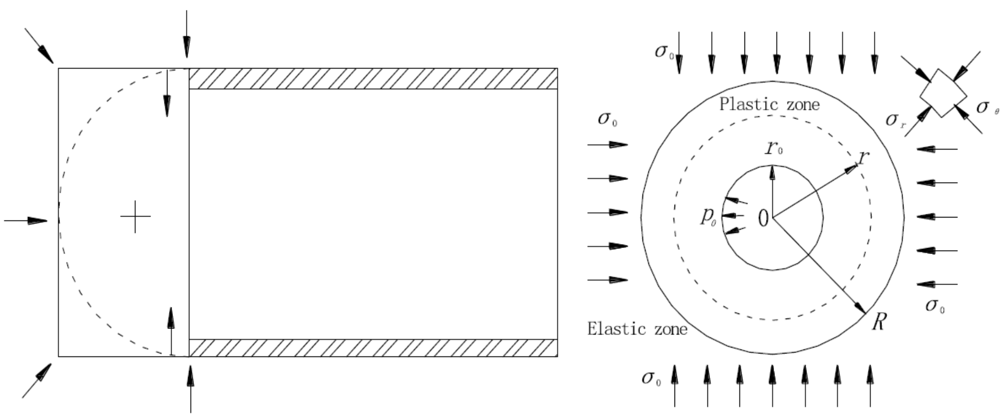

Fig. 1 Circular opening in an infinite medium.

2. Theory and methodology

2.1 Cavity contraction

The analysis model presented by Yu (2000) is adopted in this study (Fig. 1). The constructions of the tunnels can be modeled using spherical or cylindrical cavity contraction, as shown in Figs. 1(a) and 1(b), respectively. The tunnels to be analyzed were constructed efficiently and positioned deep in the ground to enable the effect of the free surface to be ignored.

Fig. 1 shows a circular opening excavated in a continuous, homogeneous, isotropic, and initially elastic rock mass subjected to hydrostatic stress (s_0). The opening surface is subjected to internal pressure (p_0). As p_0 gradually decreased, radial displacement occurred, and a plastic region developed around the opening when p_0 was less than p_{1y} (i.e., the initial yielding stress). r_0 and R are the radii of the circular opening and the elastic-plastic interface, respectively, and s_r and s_q are the radial and circumferential stresses, respectively.

2.2 Assumptions

Several assumptions have been made to determine the influences of seepage force and out-of-plane stress. The rock mass around the cavity contracting and circular opening is regarded as an isotropic, continuous, and permeable medium. In the seepage force analyses, the axisymmetric condition is not considered. Thus, pore water pressure is computed as a function of radial distance (r). Because of the complex solution of pore pressure in an arbitrary direction, the proposed solution considers only the pore pressure through the radial direction in this paper. The rock masses around the circular opening adhere to the generalized H-B failure criterion under the plane strain condition. The strain constitutive model that follows a non-associated flow rule is employed for formula derivation. The elastic strain in the plastic and softening regions of the surrounding rock accords with Hooke’s law. Compressive stress and direct strain are regarded as positive throughout the process. When the effects of seepage force and out-of-plane stress are taken into account, the solution differs from those for the normal plane strain problem.

According to the literatures in Reed (1988), Pan and Brown (1996), Lu *et al.* (2010) and Wang *et al.* (2012a, b), $s_z=q$ in the elastic region. In the plastic region, $s_q=s_z$ at the tunnel wall. If the tunnel support pressure is reduced below the critical value, an inner plastic zone will develop in which $s_q \le s_z$. Therefore, in order to the influences of the out-of-plane stress and seepage force on cavity contracting and tunnel opening, three cases of the out-of-plane stress being the minor, intermediate, or major principal stress are assumed separately.

2.3 Generalized Hoek-Brown failure criterion

The generalized Hoek-Brown failure criterion can be written as follows (Yang and Pan 2015, Yang and Yan 2015, Yang *et al.* 2016, Yang and Yin 2010)

$$\sigma_1 - \sigma_3 = \sigma_c \left(m\frac{\sigma_3}{\sigma_c} + s\right)^n \tag{1}$$

where, s_c is the unconfined compressive strength of the rock mass and s_1 and s_3 are the major and minor principal stresses, respectively. *m*, *s*, and *n* are the H-B constants for the rock mass before yielding, which are expressed as follows

$$m = m_i \exp\left(\frac{GSI - 100}{28 - 14D}\right) \tag{2}$$

$$S = \exp\left(9\frac{GSI - 100}{28 - 3D}\right) \tag{3}$$

$$n = \frac{1}{2} + \frac{1}{6}\left[\exp\left(-\frac{GSI}{15}\right) - \exp\left(-\frac{20}{3}\right)\right] \tag{4}$$

where, *D* is a factor that depends on the degree of disturbance to which the rock has been subjected to in terms of blast damage and stress relaxation, which varies between 0 and 1 and GSI is the geological strength index (GSI) of the rock mass, which varies between 10 and 100.

For the contracting cavities and tunnel opening with unloading condition, s_1=s_q and s_3=s_r, and Eq. (1) can be expressed as follows

$$\sigma_\theta = \sigma_r + \sigma_c\left(m\frac{\sigma_r}{\sigma_c} + s\right)^n \tag{5}$$

The radial stress (s_r) at the elastic–plastic interface can be determined using the Newton-Raphson method with Eq. (6)

$$\sigma_R = \sigma_0 - \frac{k}{k+1}\sigma_c\left(m\frac{\sigma_R}{\sigma_c} + s\right)^n \tag{6}$$

where s_0 is the hydrostatic in situ stress at infinity, and *k*=1 and *k*=2 are the cylindrical and spherical contraction cavity problems, respectively.

Eq. (6) is applicable only to the case of a deep tunnel excavated through a material that features an initial isotropic stress state.

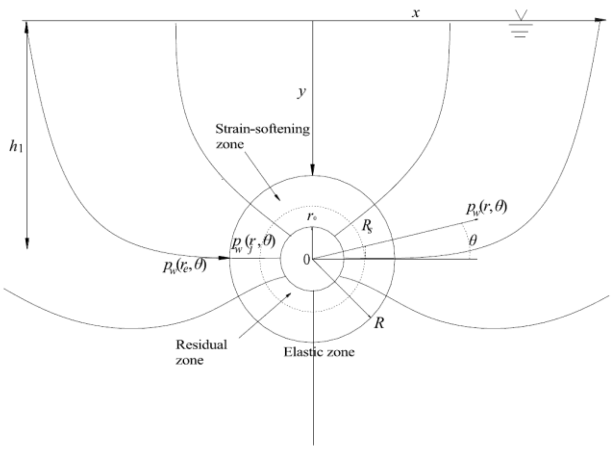

Fig. 2 Seepage flow net in different regions around the opening (Fahimifar and Zareifard 2009)

2.4 Seepage force

The circular opening excavated below the groundwater table with a constant hydraulic head is depicted in Fig. 2. Pore pressure is determined using Bernoulli's equation based on the steady state of the flow effect and on the datum level at the tunnel depth. The flow net of radial seepage is developed in the plastic zone. The tunnel cross-section and the boundary between the elastic and plastic zones are considered to be circular. Thus, ratio r_e/h_1 should be reasonably small to achieve acceptable results. Inward seepage flow rate (q) is assumed to be positive.

Fig. 2 shows that the water head (h_a) acts on the wall of the circular tunnel with inner radius (r_0). The water head of hydrostatic pressure (h_0) is far from this wall. The hydraulic conductivity of the surrounding rock is assumed to be similar in all directions. Seepage flows mainly along the radial direction in the considered tunnel range. Thus, the continuity seepage differential equation based on that developed by Bear (1988) can be written as

$$\frac{\partial^2 H}{\partial r^2} + \frac{1}{r}\frac{\partial H}{\partial r} = 0 \tag{7}$$

In this equation, $H(r)_{r=r_0} = h_a$ and $H(r)_{r\to\infty} = h_0$ are the boundary conditions. This formula has no solution; however, it can be solved by replacing the second condition ($H(r)_{r\to\infty} = h_0$) with $H(r)_{r=\alpha r_0} = h_a$. Therefore, the solution of Eq. (8) is

$$H = \frac{1}{\ln\alpha}\left(h_a \ln\frac{\alpha\, r_0}{r} + h_0 \ln\frac{r}{r_0}\right) \tag{8}$$

where, a is a constant of seepage force. The equation can be assigned a conveniently large value if it satisfies the required engineering accuracy. According to Li *et al.* (2004), this requirement can be sufficiently met at a=30.

In the axisymmetric plane strain problem, seepage force refers to volume force and is obtained using Eq. (9)

$$F_r = -\gamma_w i = -\gamma_w \frac{d(\xi H)}{dr} = \frac{\gamma_w \xi (h_a - h_0)}{r \ln\alpha} \tag{9}$$

where, i is the hydraulic gradient; x is the effective coefficient of pore water pressure in the rock mass; H is the water-level fluctuation; a is the constant of seepage force; g_w is the unit weight of water; r is the radial distance from the center of the opening; and h_0 and h_a are the initial and final water levels, respectively.

2.5 Stress and displacement in the elastic region

Equilibrium equation and stress boundary conditions. The axisymmetric equilibrium equation for the elements of rock mass in polar coordinates, including seepage body force (F_r), is given by

$$\frac{d\sigma_r}{dr} + k\frac{\sigma_r - \sigma_\theta}{r} + F_r = 0 \tag{10}$$

where, r is the radial distance from the center of the opening, s$_r$ and s$_q$ are the radial and circumferential stress, and *k* denotes the cylindrical (*k*=1) and spherical cases (*k*=2), respectively.

The two boundary conditions for the problem are as follows.

$$\sigma_r \big|_{r=R} = \sigma_R \tag{11}$$

$$\lim_{r\to\infty} \sigma_r = \sigma_0 \tag{12}$$

As a tunnel is excavated, radial stress at the tunnel boundary decreases from the initial value (s_0), and the deformation of the rock is initially purely elastic. Under conditions of radial symmetry, the elastic stress-strain relationship for the case of cylindrical and spherical cavity contractions can be expressed as follows

$$\begin{cases} \varepsilon_r^e = \dfrac{1}{E}\left[(\sigma_r - \sigma_0) - \mathrm{k}\,\nu(\sigma_\theta - \sigma_0)\right] \\ \varepsilon_\theta^e = \dfrac{1}{E}\left\{[1-(k-1)\nu](\sigma_\theta - \sigma_0) - \nu(\sigma_r - \sigma_0)\right\} \end{cases} \tag{13}$$

where, *E* is Young's modulus, and n is the Poisson's ratio of the rock mass.

If Eq. (13) is substituted into Eq. (10), the following can be obtained

$$\frac{d^2u}{dr^2}[1-(k-1)v] + \frac{1}{r}\frac{du}{dr} - \frac{u}{r^2} = -F_r \frac{(1+v)(1-kv)}{E} \tag{14}$$

The solution of stress for the case of *k*=1 can be easily obtained

$$\begin{aligned} \sigma_r &= \sigma_0 + \gamma_w \xi(h_a - h_0) + \frac{\gamma_w \xi(h_a - h_0)}{2(1-v)\ln\alpha} \ln\frac{r}{b} \\ &+ \frac{R^2}{R^2 - b^2}\left(\frac{b^2}{r^2} - 1\right)\left[\sigma_0 + \gamma_w \xi(h_a - h_0) - \sigma_R + \frac{\gamma_w \xi(h_a - h_0)}{2(1-v)\ln\alpha}\ln\frac{R}{b}\right] \end{aligned} \tag{15}$$

$$\begin{aligned} \sigma_\theta &= \sigma_0 + \gamma_w \xi(h_a - h_0) + \frac{\gamma_w \xi(h_a - h_0)}{2\ln\alpha}\left[\frac{\ln(r/b)}{1-v} + \frac{2v-1}{1-v}\right] \\ &- \frac{R^2}{R^2 - b^2}\left(\frac{b^2}{r^2} - 1\right)\left[\sigma_0 + \gamma_w \xi(h_a - h_0) - \sigma_R + \frac{\gamma_w \xi(h_a - h_0)}{2(1-v)\ln\alpha}\ln\frac{R}{b}\right] \end{aligned} \tag{16}$$

If Eqs. (5) and (14) are combined with the boundary conditions of Eqs. (11) and (12), the displacement field in the elastic zone is determined by the following equation

$$\frac{u}{r} = \frac{1}{2G}\left\{ \begin{aligned} &(1-2v)\gamma_w \xi(h_a - h_0) + (1-2v)\frac{\gamma_w \xi(h_a - h_0)}{2\ln\alpha}\left[\frac{\ln(r/b)}{1-v} - 1\right] \\ &- \frac{R^2}{R^2 - b^2}\left(\frac{b^2}{r^2} + 1 - 2v\right)\left[\sigma_0 + \gamma_w \xi(h_a - h_0) - \sigma_R + \frac{\gamma_w \xi(h_a - h_0)}{2(1-v)\ln\alpha}\ln\frac{R}{b}\right] \end{aligned} \right\} \tag{17}$$

The solution of stress for the case of k=2 can also be obtained

$$\sigma_r = \sigma_0 + \frac{(1+v)\gamma_w \xi (h_a - h_0)}{(v-2)\ln\alpha}\ln\frac{r}{b} + \left[\sigma_R - \sigma_0 - \frac{(1+v)\gamma_w \xi (h_a - h_0)}{(v-2)\ln\alpha}\ln\frac{R}{b}\right]\left(\frac{r}{R}\right)^{\frac{2-v}{v-1}} \tag{18}$$

$$\begin{aligned}\sigma_\theta = \sigma_0 &+ \frac{(1+v)\gamma_w \xi (h_a - h_0)}{(v-2)\ln\alpha}\ln\frac{r}{b} - \frac{(1-2v)\gamma_w \xi (h_a - h_0)}{(v-2)\ln\alpha} \\ &+ \frac{1}{(v-1)}\left[\sigma_R - \sigma_0 - \frac{(1+v)\gamma_w \xi (h_a - h_0)}{(v-2)\ln\alpha}\ln\frac{R}{b}\right]\left(\frac{r}{R}\right)^{\frac{2-v}{v-1}}\end{aligned} \tag{19}$$

$$\frac{u}{r} = \frac{1}{2G}\left\{\begin{aligned}&\frac{(1-2v)\gamma_w \xi (h_a - h_0)}{(2-v)\ln\alpha}\left[\ln\frac{b}{r} + \frac{(1-v)}{(1+v)}\right] \\ &-\left[(\sigma_R - \sigma_0) - \frac{(1+v)\gamma_w \xi (h_a - h_0)}{(v-2)\ln\alpha}\ln\frac{R}{b}\right]\left(\frac{r}{R}\right)^{\frac{2-v}{v-1}}\end{aligned}\right\} \tag{20}$$

2.6 Stress and displacement in the plastic region

(1) Stress

Substituting Eq. (5) into Eq. (10) leads to the following

$$\frac{d\sigma_r}{dr} - k\frac{\sigma_c\left(m\frac{\sigma_r}{\sigma_c} + s\right)^n}{r} + F_r = 0 \tag{21}$$

Given that Eq. (21) is a non-linear differential equation, only a numerical solution can be obtained with the boundary conditions: $\sigma_r\big|_{r=r_0} = p_i$ and $\sigma_r\big|_{r\to\infty} = \sigma_0$.

When seepage force is not considered, the solution of Eq. (18) can be expressed as follows

$$\sigma_r = \frac{\sigma_c}{m}\left\{\left[\left(m\frac{p_0}{\sigma_c} + s\right)^{1-n} + km(1-n)\ln\left(\frac{r}{r_0}\right)\right]^{\frac{1}{1-n}} - s\right\} \tag{22}$$

where, r_0 is the radius of the tunnel opening and p_0 is the uniformly distributed support or fluid pressure in the radial direction along the opening surface.

If Eq. (22) is substituted into Eq. (5), circumferential stress is obtained as F_r=0.

If Eq. (22) is solved with the boundary condition ($\sigma_r\big|_{r=R} = \sigma_R$), the plastic radius can be given by

$$R = r_0\exp\left\{\frac{1}{km(1-n)}\left[\left(m\frac{\sigma_r}{\sigma_c} + s\right)^{1-n} - \left(m\frac{p_0}{\sigma_c} + s\right)^{1-n}\right]\right\} \tag{23}$$

For the special case of k=1, Eqs. (22) and (23) are simplified to Eqs. (24) and (25)

$$\sigma_r = \frac{\sigma_c}{m}\left\{\left[\left(m\frac{p_i}{\sigma_c}+s\right)^{1-n} + m(1-n)\ln\left(\frac{r}{r_0}\right)\right]^{\frac{1}{1-n}} - s\right\} \tag{24}$$

$$R = a\exp\left\{\frac{1}{m(1-n)}\left[\left(m\frac{\sigma_R}{\sigma_c}+s\right)^{1-n} - \left(m\frac{p_i}{\sigma_c}+s\right)^{1-n}\right]\right\} \tag{25}$$

Eqs. (24) and (25) were also obtained by Sharan (2008).

(2) Displacement

In the plastic region, radial and circumferential strain can be decomposed as follows

$$\varepsilon_r = \varepsilon_r^e + \varepsilon_r^p \tag{26}$$

$$\varepsilon_\theta = \varepsilon_\theta^e + \varepsilon_\theta^p \tag{27}$$

where, the superscripts e and p represent the elastic and plastic parts, respectively.

Based on Wang's theory, the strain equilibrium equation is given by

$$\frac{d\varepsilon_\theta}{dr} + k\frac{\varepsilon_\theta - \varepsilon_r}{r} = 0 \tag{28}$$

If Eqs. (26) and (27) are substituted into Eq. (28), Eq. (28) is rewritten as

$$\frac{d\varepsilon_\theta^p}{dr} + k\frac{\varepsilon_\theta^p - \varepsilon_r^p}{r} = -\frac{d\varepsilon_\theta^e}{dr} - k\frac{\varepsilon_\theta^e - \varepsilon_r^e}{r} \tag{29}$$

Elastic strain is assumed to be relatively small compared with plastic strain in the plastic region, and hence, elastic strain can be neglected. Following the non-associated flow rule, the plastic parts of the radial and circumferential strains can be expressed as follows

$$k\varepsilon_r^p + h\varepsilon_\theta^p = 0 \tag{30}$$

where, parameter h is a function of the dilation angle (j) and is given by h = (1+sin j)/(1-sin j).

Substituting Eq. (21) into Eq. (13) results in the following

$$\frac{d\varepsilon_\theta^e}{dr} = \frac{1}{E}\left((1-kv)+[1-(k-1)v]nm\left(m\frac{\sigma_r}{\sigma_c}+s\right)^{n-1}\right)\left[k\frac{\sigma_c\left(m\frac{\sigma_r}{\sigma_c}+s\right)^n}{r} - F_r\right]. \tag{31}$$

Substituting Eq. (31) into Eq. (29) leads to the following

$$\frac{d\varepsilon_\theta^p}{dr} + k\frac{(1+h/k)\varepsilon_\theta^p}{r} = f(r) \tag{32}$$

where

$$f(r)=-\frac{1}{E}\left((1-kv)+[1-(k-1)v]nm\left(m\frac{\sigma_r}{\sigma_c}+s\right)^{n-1}\right)\left[k\frac{\sigma_c\left(m\frac{\sigma_r}{\sigma_c}+s\right)^n}{r}-F_r\right]-k\frac{1+v}{E}\frac{\sigma_c\left(m\frac{\sigma_r}{\sigma_c}+s\right)^n}{r} \tag{33}$$

If Eq. (32) is solved, the plastic strain is

$$\varepsilon_\theta^p=r^{-k(1+h/k)}\int r^{k(1+h/k)}f(r)dr+c_1r^{-k(1+h/k)} \tag{34}$$

where, c_1 is the integration constant.

Because the plastic strain at $r=R$ is equal to the difference ($\Delta\varepsilon^e_\theta$) of the elastic strain in the elastic and plastic regions for the proposed model, the following equation can be derived

$$\Delta\varepsilon_\theta^e-\Delta\varepsilon_\theta^p\Big|_{r=R}=\frac{1}{R^{h(h/k+1)}}\int^R r^{k(1+h/k)}f(r)dr+c_1R^{k(1+h/k)} \tag{35}$$

The integration constant c_1 can be determined by

$$c_1=-\int^R r^{k(1+h/k)}f(r)dr+R^{k(1+h/k)}\Delta\varepsilon_\theta^e \tag{36}$$

In which the circumferential strain increment ($\Delta\varepsilon^e_\theta$) in the elastic region is expressed as

$$\varepsilon_\theta^e=\frac{1}{E}\{[1-(k-1)v](\sigma_\theta-\sigma_0)-v(\sigma_r-\sigma_0)\} \tag{37}$$

The circumferential strain (ε^{er}_θ) in the plastic region is given by the following equation

$$\varepsilon_\theta^{er}=\frac{1}{E}\{[1-(k-1)v](\sigma_{\theta r}-\sigma_0)-v(\sigma_r-\sigma_0)\} \tag{38}$$

And only the elastic part can be obtained by Eq. (38).

The expression of $\Delta\varepsilon^e_\theta$ is given by

$$\Delta\varepsilon_\theta^e=\varepsilon_\theta^e-\varepsilon_\theta^{er}=\frac{1-(k-1)}{E}(\sigma_\theta-\sigma_{\theta r})=\frac{1-(k-1)}{E}\left[\sigma_c\left(m\frac{\sigma_r}{\sigma_c}+s\right)^n-\sigma_{cr}\left(m_r\frac{\sigma_r}{\sigma_{cr}}+s_r\right)^{n_r}\right] \tag{39}$$

If Eq. (39) is substituted into Eq. (36), the constant c_1 is

$$c_1=-\int^R r^{k(h/k+1)}f(r)dr+R^{k(h/k+1)}\frac{1-(k-1)}{E}\left[\sigma_c\left(m\frac{\sigma_r}{\sigma_c}+s\right)^n-\sigma_{cr}\left(m_r\frac{\sigma_r}{\sigma_{cr}}+s_r\right)^{n_r}\right] \tag{40}$$

The radial displacement can be obtained by the following

$$\frac{u}{r}=\frac{1}{r^{k(h/k+1)}}\int_R^r r^{k(h/k+1)}f(r)dr+\left(\frac{R}{r}\right)^{k(h/k+1)}\Delta\varepsilon_\theta^e+\frac{1}{E}\left\{(1-kv)(\sigma_r-\sigma_0)+[1-(k-1)v]\sigma_c\left(m\frac{\sigma_r}{\sigma_c}+s\right)^n\right\} \tag{41}$$

For the special case of k=1, Eq. (31) can be reduced to the following equation

$$\frac{d\varepsilon_\theta^e}{dr}=\frac{1}{E}\left((1-v)+nm\left(m\frac{\sigma_r}{\sigma_c}+s\right)^{n-1}\right)\left[k\frac{\sigma_c\left(m\frac{\sigma_r}{\sigma_c}+s\right)^n}{r}-F_r\right] \tag{42}$$

For the special case of k=1 and F_r=0, Eqs. (31) and (33) are reduced into Eqs. (43) and (44) as follows

$$f(r)=-\frac{1}{E}\left((1-v)+nm\left(m\frac{\sigma_r}{\sigma_c}+s\right)^{n-1}\right)\frac{\sigma_c\left(m\frac{\sigma_r}{\sigma_c}+s\right)^n}{r}-\frac{1+v}{E}\frac{\sigma_c\left(m\frac{\sigma_r}{\sigma_c}+s\right)^n}{r} \tag{43}$$

$$\frac{d\varepsilon_\theta^e}{dr}=\frac{1}{E}\left((1-v)+nm\left(m\frac{\sigma_r}{\sigma_c}+s\right)^{n-1}\right)\frac{\sigma_c\left(m\frac{\sigma_r}{\sigma_c}+s\right)^n}{r} \tag{44}$$

3. Solutions

3.1 Stress in the elastic region

Only the plain strain problem is evaluated considering the effect of out-of-plane stress for the solutions of tunnel. The following discussion in this section is the case of k=1 and k=2.

The elastic strain that considers the effect of the out-of-plane stress in the elastic region is

$$\begin{cases}\varepsilon_r^e=\dfrac{1}{E}\left[\sigma_r-v(\sigma_\theta+\sigma_z)-(\sigma_0-v\sigma_0-vq)\right]\\ \varepsilon_\theta^e=\dfrac{1}{E}\left[\sigma_\theta-v(\sigma_r+\sigma_z)-(\sigma_0-v\sigma_0-vq)\right]\\ \varepsilon_z^e=\dfrac{1}{E}\left[\sigma_z-v(\sigma_\theta+\sigma_r)-(q-2v\sigma_0)\right]\end{cases} \tag{45}$$

where, q is the out-of-plane stress along the axis of the tunnel.

In the elastic region, s_z=q, therefore, the radial and circumferential stresses are the same as in Eqs. (18) and (19).

Displacement in the elastic region is

$$u=\frac{r}{E}\left[\sigma_\theta-v\sigma_r-(1-v)\sigma_0\right] \tag{46}$$

3.2 Stress and strain in the plastic region (σ_z-the major principal stress)

The generalized H-B failure criterion can be expressed as follows

$$\sigma_z = \sigma_r + \sigma_c \left(m \frac{\sigma_r}{\sigma_c} + s \right)^n \tag{47}$$

The boundary condition at the interface between the plastic and elastic regions is s_z=*q*. Using the boundary condition and Eq. (47), the radial stress at the interface between the plastic and elastic region can be derived as

$$q = p_{c1} + \sigma_c \left(m \frac{p_{c1}}{\sigma_c} + s \right)^n \tag{48}$$

where, p_{c1} is the critical internal pressure and *q* is the major principal stress.
The non-associate flow rule is

$$\begin{cases} k\varepsilon_r^p + h\varepsilon_z^p = 0 \\ \varepsilon_\theta^p = 0 \end{cases} \tag{49}$$

Combining Eqs. (28), (45), and (49) results in the following

$$r\left(\frac{d\sigma_\theta}{dr} - v\frac{d\sigma_r}{dr} - v\frac{d\sigma_z}{dr} \right) = -\left(k + kv + vh\right)\sigma_\theta + \left(k + kv - vh\right)\sigma_r + h\sigma_z - h\left(q - 2v\sigma_0\right) \tag{50}$$

s_z, s_q, and s_r can be solved using Eqs. (10), (47), and (50).
If Eqs. (10) and (47) are substituted into Eq. (50), the differential equation is

$$\begin{aligned} &\frac{r^2}{k}\frac{d^2\sigma_r}{dr^2} + \left(2 + \frac{1}{k} - v + \frac{vh}{k}\right) r \frac{d\sigma_r}{dr} - vnm\left(m\frac{\sigma_r}{\sigma_c} + s \right)^{n-1} r\frac{d\sigma_r}{dr} + h\left(2v - 1\right)\sigma_r \\ &-h\sigma_c\left(m\frac{\sigma_r}{\sigma_c} + s \right)^n + h\left(q - 2v\sigma_0\right) + \left(1 + v + \frac{vh}{k}\right)\frac{\gamma_w \xi\left(h_a - h_0\right)}{\ln\alpha} = 0 \end{aligned} \tag{51}$$

and

$$\frac{u}{r} = \varepsilon_\theta = \varepsilon_\theta^e = \frac{1}{E}\left[\sigma_\theta - v\left(\sigma_z + \sigma_r\right) - \left(\sigma_0 - v\sigma_0 - vq\right)\right] \tag{52}$$

Substituting Eqs. (10) and (47) into Eq. (52) leads to

$$u = \frac{r}{E}\left[\frac{r}{k}\frac{d\sigma_r}{dr} - v\sigma_c\left(m\frac{\sigma_r}{\sigma_c} + s \right)^n + \left(1 - 2v\right)\sigma_r - \left(\sigma_0 - v\sigma_0 - vq\right) + \frac{\gamma_w \xi\left(h_a - h_0\right)}{k\ln\alpha} \right] \tag{53}$$

In the inner plastic zone $\left(r_0 < r < \overline{R}\right), \sigma_z = \sigma_\theta > \sigma_r$.

$$u = r^{-h}\int_{\bar{R}}^{r} r^{h} f\left(r\right)dr + u_{\bar{R}}\left(\frac{u_{\bar{R}}}{r}\right)^{h} \tag{54}$$

where, $f\left(r\right)=\varepsilon_{r}^{e}+h\varepsilon_{\theta}^{e}+\frac{h}{k}\varepsilon_{z}^{e}$.

As $r=R$ and $u=u_c$, then

$$u_{c1} = \frac{R}{2G}\left\{\sigma_0 - p_{c1} + \frac{\gamma_w \xi\left(h_a - h_0\right)}{2\ln\alpha}\left[2\ln\left(\frac{R}{b}\right) + 4\left(1-v\right)\ln\alpha - \left(1-2v\right)\right]\right\} \tag{55}$$

Plastic radius can be determined using Eqs. (53), (54) and (55). Stress (s_z, s_q, and s_r) in the plastic region can be obtained using Eqs. (10), (47), and (51), whereas displacement can be obtained using Eq. (53) and (54) with the boundary conditions: $s_r(r=r_0)=p_{in}$, $s_r(r=R)=p_{c1}$, and $u(r=R)=u_{c1}$.

3.3 Stress and strain in the plastic region (σ_z−the intermediate principal stress)

The radial and circumferential stresses in the plastic region can be solved using Eq. (21). The out-of-plane stress is

$$\sigma_z = v\left(\sigma_\theta + \sigma_r\right) - 2v\sigma_0 + q \tag{56}$$

Considering the effects of out-of-plane stress, the elastic strain in the elastic region can be given by

$$\varepsilon_{\theta}^{e} = \frac{1}{E}\left[\left(1-v-2v^2\right)\left(\sigma_r - \sigma_0\right) + \left(1-v^2\right)\sigma_c\left(m\frac{\sigma_r}{\sigma_c}+s\right)^{n}\right] \tag{57}$$

The plastic strain is the same as in Eq. (34), which is as follows

$$\begin{aligned} f(r) = -\frac{1}{E}&\left(\left(1-v-2v^2\right)+\left(1-v^2\right)nm\left(m\frac{\sigma_r}{\sigma_c}+s\right)^{n-1}\right) \\ &\times\left[k\frac{\sigma_c\left(m\frac{\sigma_r}{\sigma_c}+s\right)^{n}}{r} - F_r\right] - k\frac{1+v}{E}\frac{\sigma_c\left(m\frac{\sigma_r}{\sigma_c}+s\right)^{n}}{r} \end{aligned} \tag{58}$$

The displacement in the plastic region is expressed as follows

$$\frac{u_r}{r} = \frac{1}{r^{(h+1)}}\int_{R}^{r} r^{(h+1)} f(r)dr + \left(\frac{R}{r}\right)^{(h+1)}\Delta\varepsilon_{\theta}^{e} + \frac{1}{E}\left[\left(1-v-2v^2\right)\left(\sigma_r-\sigma_0\right)+\left(1-v^2\right)\sigma_c\left(m\frac{\sigma_r}{\sigma_c}+s\right)^{n}\right] \tag{59}$$

Eqs. (15), (16), (17), (21), and (59) show that the plastic radius and stress in the elastic and plastic regions are unaffected by out-of-plane stress in the plane strain condition because out-of-plane is the intermediate principal stress, except for the displacement in the plastic region.

3.4 Stress and strain in the plastic region (σ_z−the minor principal stress)

The generalized H-B failure criterion is expressed as follows

$$\sigma_\theta = \sigma_z + \sigma_c \left(m \frac{\sigma_z}{\sigma_c} + s \right)^n \tag{60}$$

The boundary condition at the interface between the plastic and elastic regions is $s_z = q$. Using the boundary condition and Eq. (60), the radial stress at the interface between the plastic and elastic regions can be derived as follows

$$p_{c3} = 2\sigma_0 - q - \sigma_c \left(m \frac{q}{\sigma_c} + s \right)^n \tag{61}$$

The non-associate flow rule is expressed as follows

$$\begin{cases} k\varepsilon_z^p + h\varepsilon_\theta^p = 0 \\ \varepsilon_r^p = 0 \end{cases} \tag{62}$$

Combining Eqs. (28), (58), and (62) results in

$$\begin{aligned} & r\left[\left(1 - \frac{k\nu}{h} \right) \frac{d\sigma_\theta}{dr} - \nu \left(1 + \frac{k}{h} \right) \frac{d\sigma_r}{dr} + \left(\frac{k}{h} - \nu \right) \frac{d\sigma_z}{dr} \right] \\ & = \left(\frac{k\nu}{h} - 1 - \nu \right) \sigma_\theta + \left(1 + \nu + \frac{k\nu}{h} \right) \sigma_r - \frac{k}{h}\sigma_z + \frac{k}{h}\left(q - 2\nu\sigma_0 \right) \end{aligned} \tag{63}$$

s_z, s_q, and s_r can be determined by combining Eqs. (10), (58), and (62). By substituting Eqs. (10) and (58) into Eq. (62) we can obtain

$$\begin{aligned} \frac{d\sigma_r}{dr} &= \frac{1}{r}\left[k\left(\sigma_z - \sigma_r \right) + k\sigma_c \left(m\frac{\sigma_z}{\sigma_c} + s \right)^n - \frac{\gamma_w \xi \left(h_a - h_0 \right)}{\ln\alpha} \right] \\ \frac{d\sigma_z}{dr} &= \left[\begin{array}{l} \sigma_r + \left(\dfrac{k^2\nu + k\nu - k}{h} - 1 - \nu + k\nu \right)\sigma_z + \left(\dfrac{k\nu + k^2\nu}{h} - 1 + k\nu - \nu \right)\sigma_c \left(m\dfrac{\sigma_z}{\sigma_c} + s \right)^n \\ + \dfrac{k}{h}\left(q - 2\nu\sigma_0 \right) - \left(\dfrac{k\nu}{h} + \nu \right)\dfrac{\gamma_w \xi \left(h_a - h_0 \right)}{\ln\alpha} \end{array} \right] \\ & \times \left[1 - \nu + \frac{k}{h} - \frac{k\nu}{h} + nm\left(1 - \frac{k\nu}{h} \right)\left(m\frac{\sigma_z}{\sigma_c} + s \right)^{n-1} \right]^{-1} r^{-1} \end{aligned} \tag{64}$$

Displacement in the plastic region is given by

$$\frac{u}{r} = \varepsilon_\theta^e + \frac{k}{h}\varepsilon_z^e = \frac{1}{E}\left[\begin{array}{l} \left(1 - \dfrac{k\nu}{h} \right)\sigma_\theta - \left(\nu + \dfrac{k\nu}{h} \right)\sigma_r + \left(\dfrac{k}{h} - \nu \right)\sigma_z \\ -\left(\sigma_0 - \nu\sigma_0 - \nu q \right) - \dfrac{k}{h}\left(q - 2\nu\sigma_0 \right) \end{array} \right] \tag{65}$$

Substitute Eq. (58) into (65) yields

$$u=\frac{r}{E}\left[\begin{array}{l}\left(1-\frac{kv}{h}\right)\sigma_c\left(m\frac{\sigma_z}{\sigma_c}+s\right)^n+\left(1-v+\frac{k}{h}-\frac{kv}{h}\right)\sigma_z-\left(v+\frac{kv}{h}\right)\sigma_r\\-\left(\sigma_0-v\sigma_0-vq\right)-\frac{k}{h}\left(q-2v\sigma_0\right)\end{array}\right] \tag{66}$$

In the inner plastic zone, $\left(r_0<r<\overline{R}\right), \sigma_\theta>\sigma_r=\sigma_z$.

$$u=r^{-h}\int_{\overline{R}}^{r} r^h f\left(r\right)dr+u_{\overline{R}}\left(\frac{u_{\overline{R}}}{r}\right)^h \tag{67}$$

where, $f\left(r\right)=\varepsilon_r^e+h\varepsilon_\theta^e+k\varepsilon_z^e$.

As $r=R$, $u=u_{c3}$ and it is expressed by

$$u_{c3}=\frac{R}{2G}\left\{\sigma_0-p_{c3}+\frac{\gamma_w\xi\left(h_a-h_0\right)}{2\ln\alpha}\left[2\ln\left(\frac{R}{b}\right)+4\left(1-v\right)\ln\alpha-\left(1-2v\right)\right]\right\} \tag{68}$$

Stress (s$_z$, s$_q$, and s$_r$), radius, and displacement in the plastic region can be determined using Eqs. (10), (64), (66), and (67) with the boundary conditions: $\sigma_r\big|_{r=r_0}=p_{in}$, $\sigma_r\big|_{r=R}=p_{c3}$, and $u=u_{c3}$.

4. Verification and application

4.1 Verification

The parameters of very good, average, and very poor rock mass were taken from published literatures (Sharan, 2008) and evaluated to determine the validity of the proposed approach, as shown in Table 1.

Fig. 3 shows that the stress distribution with the proposed approach corresponds to a=5 m, a=30, h_0=0, h_a=50 m, x=1, and p_0=1.0 MPa for very good, average, and very poor rock masses, respectively. The results in this figure and in the subsequent figures were obtained with the same proposed approach.

Fig. 3 shows that the effects of seepage force on the radial and circumferential stresses were not obvious for very good rock mass, and results of stress for $F_r\neq0$ were less than those for F_r=0. The effect of seepage force on stress were found to be more significant when rock mass is poorer.

The effects of seepage force on R/r_0 with different GSI values are shown in Fig. 4.

Fig. 4 shows that the magnitude of R/r_0 for $F_r\neq0$ was larger than that for F_r=0. The effects of seepage force on plastic radius were more significant when rock mass was poorer.

Displacement distributions that consider the effects of seepage force are shown in Fig. 5 for very good, average, and very poor rock mass, respectively.

Fig. 5 shows that the effect of seepage force on displacement was more obvious, and that the displacement for $F_r\neq0$ was larger than those for F_r=0. The effect of seepage force on the displacement was smaller when the rock mass was of better quality.

The effects of h_a on the displacement and plastic radius of different rocks are shown in Figs. 6 and 7.

Table 1 Basic properties of rock mass used in numerical tests

Rock example	Reference	Quality of rock mass	n	s_{ci} (MPa)	E(GPa)	n	m_i	s_0(MPa)
A	Sharan (2008)	Very good	0.500911	150	42	0.2	25	200
B		Average	0.505734	80	9	0.25	12	50
C		Very poor	0.522344	20	1.4	0.3	8	12

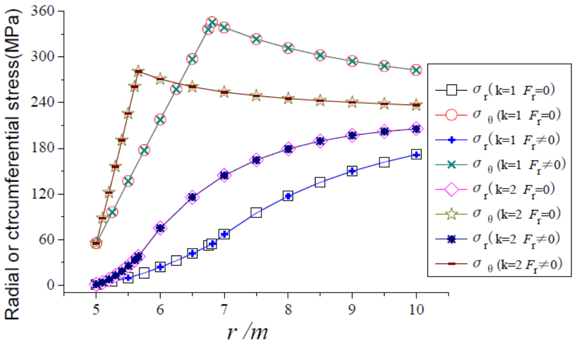

(a) Very good rock mass

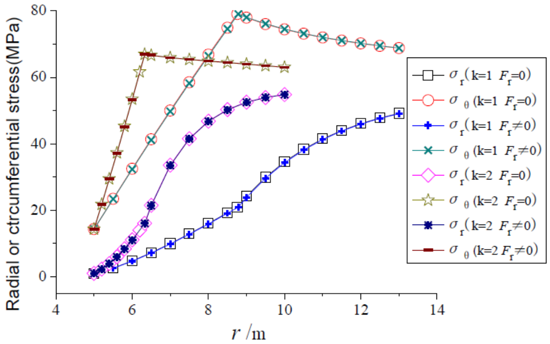

(b) Average rock mass

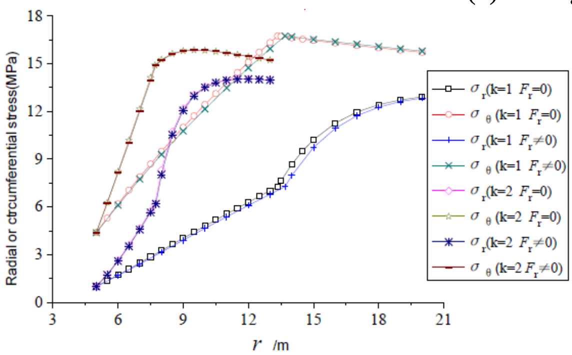

(c) Very poor rock mass

Fig. 3 Effects of F_r on stress

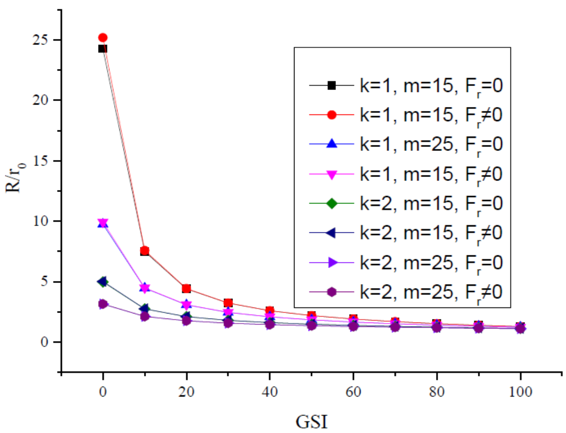

Fig. 4 Effects of F_r on R / r_0 with increasing parameters of GSI

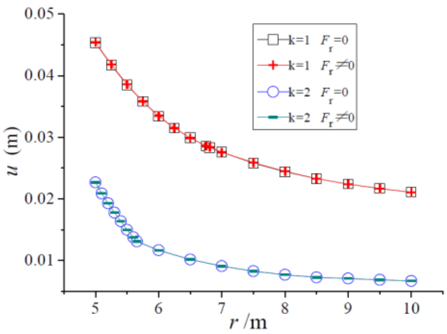

(a) Very good rock mass

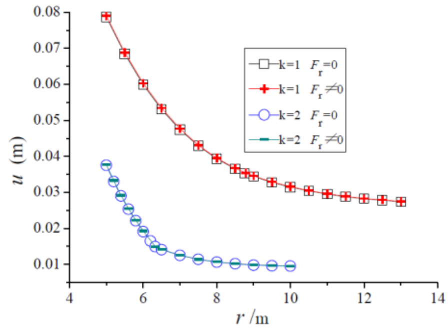

(b) Average rock mass

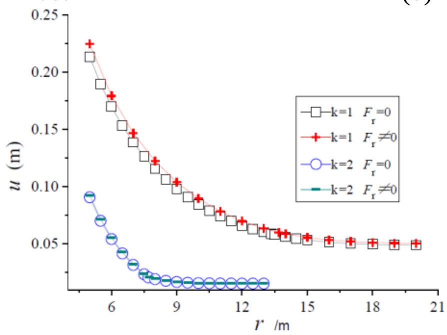

(c) Very poor rock mass

Fig. 5 Effects of F_r on displacement with increasing radius

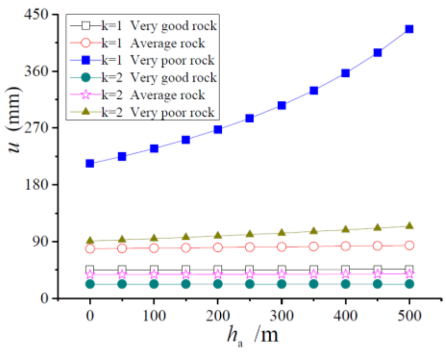

Fig. 6 Effects of h_a on displacement for different rocks

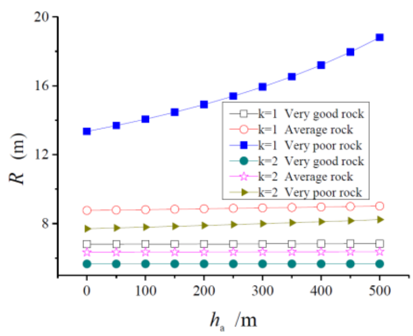

Fig. 7 Effects of h_a on plastic radii for different rocks

Table 2 Radii of plastic zone and displacement of surrounding rock

q(MPa)	R/r_0[a]	R'/r_0[b]	Difference (%)	u/r[a]	u'/r[b]	Difference (%)
50.00	1.8660	1.7022	9.62	1.1570	1.1271	2.65
44.16	1.6516	1.5937	3.63	1.0863	1.0791	0.67
35.00	1.6516	1.5937	3.63	1.0479	1.0368	1.07
22.50	1.6516	1.5937	3.63	1.0406	1.0275	1.27
15.83	1.6516	1.5937	3.63	1.0420	1.0275	1.41
15.00	1.7591	1.5937	10.38	1.0422	1.0275	1.43

a: Results calculated by the Hoek-Brown criterion

b: Results calculated by using equation of Fenner

Table 3 Displacement that considers the out-of-plane stress (k=1)

out-of-plane stress q (MPa)		Rock example	Radius of plastic zone $R(m)$	Displacement considering σ_z (m)	Differences	Radius of plastic zone $R(m)$	Displacement considering σ_z and F_r (m)	Differences
Major principal stress	400	A	7.2116	0.0498 (0.0453)	9.93%	7.2141	0.0499 (0.0454)	9.91%
	100	B	10.6913	0.0905 (0.0787)	15.00%	10.7263	0.0912 (0.0791)	15.30%
	20	C	17.7536	0.2348 (0.2135)	9.98%	18.297	0.2489 (0.2248)	10.72%
Intermediate principal stress	100	A	6.807	0.0447 (0.0453)	1.32%	6.810	0.0447 (0.0454)	1.54%
	25	B	8.760	0.0759 (0.0787)	3.56%	8.783	0.0763 (0.0791)	3.54%
	10	C	13.347	0.1989 (0.2135)	6.84%	13.689	0.2094 (0.2248)	6.85%
Minor principal stress	50	A	7.2121	0.0445 (0.0453)	1.77%	7.2146	0.0445 (0.0454)	1.98%
	15	B	12.7355	0.0758 (0.0787)	3.68%	12.7846	0.0764 (0.0791)	3.41%
	7	C	14.0329	0.1996 (0.2135)	6.51%	14.4040	0.2104 (0.2248)	6.41%

Table 4 Displacement that considers the out-of-plane stress (k=2)

out-of-plane stress q(MPa)		Rock example	Radius of plastic zone $R(m)$	Displacement considering σ_z (m)	Differences	Radius of plastic zone $R(m)$	Displacement considering σ_z and F_r (m)	Differences
Major principal stress	400	A	6.005	0.0318 (0.0227)	40.09%	6.0056	0.0318 (0.0227)	40.09%
	100	B	7.3173	0.0429 (0.0375)	14.40%	7.3232	0.0430 (0.0377)	14.06%
	20	C	9.4361	0.0748 (0.09078)	17.60%	9.5068	0.0767 (0.09267)	17.23%

Table 4 Continued

out-of-plane stress $q(MPa)$		Rock example	Radius of plastic zone $R(m)$	Displacement considering σ_z (m)	Differences	Radius of plastic zone $R(m)$	Displacement considering σ_z and F_r (m)	Differences
Intermediate principal stress	100	A	5.655	0.0259 (0.0227)	14.10%	5.656	0.0259 (0.0227)	14.10%
	25	B	6.328	0.0428 (0.0375)	14.13%	6.333	0.0430 (0.0377)	14.06%
	10	C	7.700	0.10217 (0.09078)	12.55%	7.745	0.10418 (0.09267)	12.42%
Minor principal stress	50	A	6.0107	0.0290 (0.0227)	27.75%	6.0112	0.0290 (0.0227)	27.75%
	15	B	8.5048	0.0264 (0.0375)	29.60%	8.5151	0.0265 (0.0377)	29.71%
	7	C	8.3904	0.0673 (0.09078)	25.86%	8.4448	0.0683 (0.09267)	26.30%

Fig. 6 shows that for very good and average rock masses, the displacement changed slightly with the increase in head pressure. The effect of h_a on the plastic radius was similar to the pattern of displacement when head pressure was involved (see Fig. 7).

To further validate the effective of the proposed approach, comparisons between the proposed approach and Fenner's solutions are carried out. The parameters of the rock example D in Sharan (2008) were adopted. The H-B parameters are converted to equivalent M-C parameters according to Hoek and Carranza-torres (2002) as f=26.87°, c=1.78 MPa. The results are shown in the Table 2.

It can be seen from Table 2 that the results of the proposed solutions are similar to those of Fenner, but the plastic zone radius and displacement of surrounding rock are larger 10.38% and 2.65% (the maximum value, respectively) than those of Fenner in the same situation. Therefore, the proposed approach tends to be more safely.

The results for different rock masses were calculated to analyze the effects of out-of-plane stress on the displacement and plastic radius (Table 3). Out-of-plane stress was considered the major, intermediate, and minor principal stresses. The results of ignoring the effects of out-of-plane stress are shown in the parentheses of Table 3.

The difference was calculated using |0.0447-0.0453|/0.0453×100%=1.32% in Table 3 and Table 4. It reveals that when out-of-plane stress was the intermediate-principal stress, displacement that considered seepage force and out-of-plane stress was greater than that when those factors were not considered. Plastic radius was also unaffected by seepage force and out-of-plane stress. The maximum difference of displacement was less than 10% with the case of k=1 and the effect is more significant when the rock has poorer mass. When k=2, the difference was larger than 10% and the effect was just contrary to k=1. Plastic radius and displacement that considered seepage force and out-of-plane stress were larger than those that only considered seepage force when the out-of-plane stress was the major stress with the case of k=2. Displacement that considered seepage force and out-of-plane stress was less than that only considered seepage force with k=1. When the out-of-plane stress was the minor-principal stress, the plastic radius that considered seepage force and out-of-plane stress were larger than those that considered only seepage force. Moreover, the displacement differences were not obvious with k=1 but varied widely when k=2.

4.2 Application of design

To confirm the validity of the proposed approach, the results of the proposed procedure and field measuring data in Baiyanshan tunnel are compared. Baiyanshan tunnel is located in Xuhuai expressway, started from Xupu County and ended in Huaihua County in Hunan Province of China. Baiyanshan tunnel has the maximum burial depth of 198 m and the length of 2390 m. The geology conditions of Baiyanshan tunnel which were monitored are illustrated in Fig. 8. The test arrangement of the sections are presented in Fig. 9. Field measuring of displacements at tunnel wall and crown was performed at several places during excavation through geodetic observations.

According to the geological investigation, laboratory experiments and inverse calculation, the basic parameters of surrounding rock are as follows: r_0=7 m, E=11 GPa, n=0.24, s_0=10 MPa, s_c=40 MPa, m=2.52, s=0.0039, f=11.74°, a=0.51, h_1=100m, x=1.

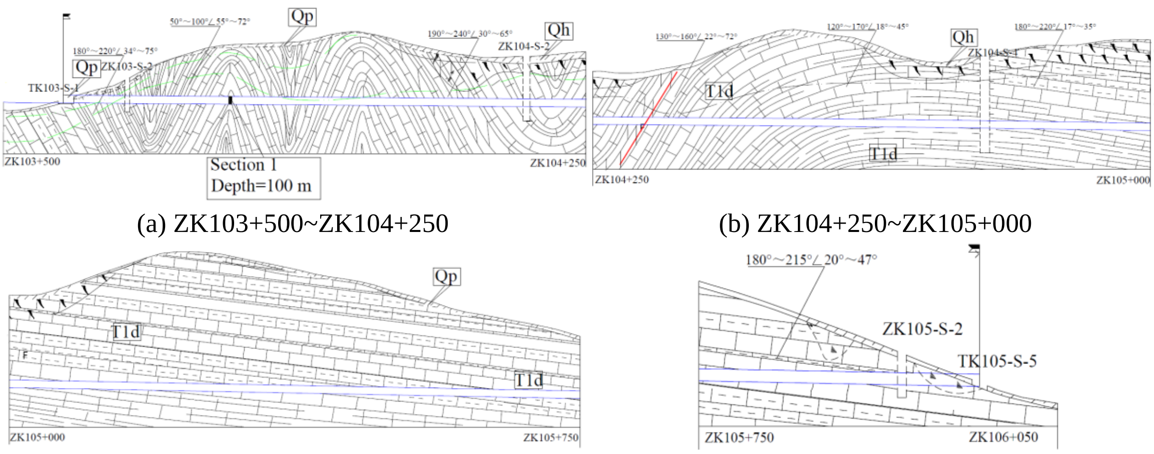

(a) ZK103+500~ZK104+250 (b) ZK104+250~ZK105+000

(c) ZK105+000~ZK105+750 (d) ZK105+750~ZK106+050

Fig. 8 Geological location of Baiyanshan tunnel.

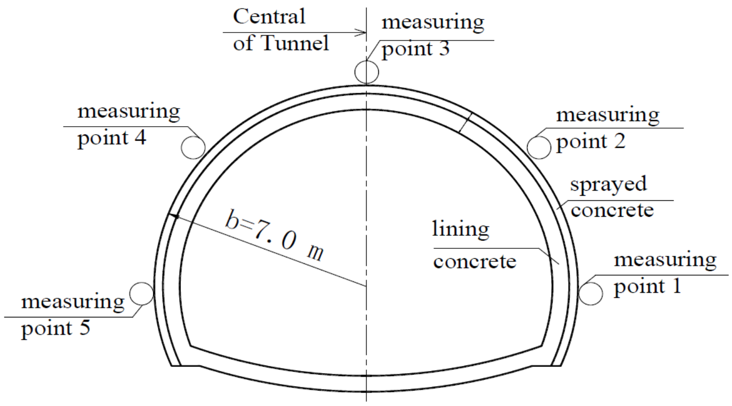

Fig. 9 Section 1 of Baiyanshan tunnel and the test arrangement

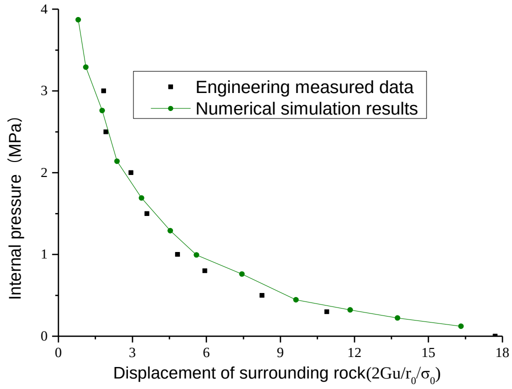

Fig. 10 The relationship between the ground response curve and the measured data

The formation curve of tunnel excavation is obtained by using the theoretical calculation method proposed in this study. The field measured data were compared with numerical simulation results as shown in as shown in Fig. 10.

It can be seen from the Fig. 10 that the ground response curves obtained by considering the seepage force and out-of-plane stress are not really accurate compared with the measured results in the field, however, the relative error is small. It is of significance to the design and construction of tunnels.

5. Conclusions

The solutions of stress, displacement, and plastic radius for spherical and cylindrical cavity contractions were proposed for the first time by considering the effects of seepage force and out-of-plane stress based on the generalized Hoek-Brown failure criterion in this study. Several examples were presented, and the following conclusions were obtained:

(1) The effects of seepage force on cavity contraction problem depend largely on the parameter selected and it were slighter when the rock mass was of better quality. Head pressure is more significant for affecting the cavity contraction, particularly when the rock mass is poor.

(2) The radial and circumferential stresses as $Fr\neq0$ were less than that as $Fr=0$, especially for very good rock mass. However, the plastic radius and displacement were larger than those considering the seepage force.

(3) In the process of solving the stresses and displacements of the tunnel in the plastic zone, it can be easily found that the influence of out-of-plane stress cannot be ignored as it serves as the major and minor principal stress when the effects of seepage force on stress and strain of a circular tunnel were considered.

(4) The proposed approach can describe the change of the stress distributions in the tunnel opening and provide reference for the design. Furthermore, when the directions of the principal tectonic stresses do not coincide with the axis of the underwater tunnel, we can apply the proposed approach in this situation to avoid the appreciable error because of ignoring the out-of-plane stress.

In summary, the proposed method could be utilized to obtain simple solutions for a wide variety of complex problems on plasticity cavity contraction in rock mechanics.

Acknowledgments

This work was supported by the National Basic Research Program of China (“973” Program, Grant No. 2013CB036004). The third author thanks the China Scholarship Council for providing him with a Ph.D. Scholarship for his research work.

References

Banerjee, S.K. and Chakraborty, D. (2016), “Seismic stability of a long unlined circular tunnel in sloping ground”, *Can. Geotech. J.*, **53**(8), 1346-1352.

Bear, J. (1988), *Dynamics of Fluids in Porous Media*, Dover Publications Inc., New York, U.S.A.

Bousbia, N. and Messast, S. (2015), “Numerical modeling of two parallel tunnels interaction using three-dimensional finite elements method”, *Geomech. Eng.*, **9**(6), 775-791.

Carranza-Torres, C. and Fairhurst, C. (1999), “The elasto-plastic response of underground excavations in rock masses that satisfy the Hoek-Brown failure criterion”, *J. Rock. Mech. Min. Sci.*, **36**(6), 777-809.

Di, H.G., Zhou, S.H., He, C., Zhang, X.H. and Luo, Z. (2016), “Three-dimensional multilayer cylindrical tunnel model for calculating train-induced dynamic stress in saturated soils”, *Comput. Geotech.*, **80**(12), 333-345.

Fahimifar, A. and Zareifard, M.R. (2009), “A theoretical solution for analysis of tunnels below groundwater considering the hydraulic-mechanical coupling”, *Tunn. Undergr. Sp. Tech.*, **24**(6), 634-646.

Fahimifar, A., Ghadami, H. and Ahmadvand, M. (2015). “The ground response curve of underwater tunnels, excavated in a strain-softening rock mass”, *Geomech. Eng.*, **8**(3), 323-359.

Huang, F., Zhu, H.H., Jiang, S.P. and Liang, B. (2016), “Excavation-damaged zone around tunnel surface under different release ratios of displacement”, *J. Geomech.*, **17**(1), 04016094

Lee, S.W., Jung, J.W., Nam, S.W. and Lee, I.M. (2006), “The influence of seepage forces on ground reaction curve of circular opening”, *Tunn. Undergr. Sp. Technol.*, **22**(1), 28-38.

Li, Z.L., Ren, Q.W. and Wang, Y.H. (2004), “Elasto-plastic analytical solution of deep-buried circle tunnel considering fluid flow field”, *Chin. J. Rock Mech. Eng.*, **23**(4), 1291-1295.

Liang, R.Z., Xia, T.D., Huang, M.S. and Lin, C.G. (2107), “Simplified analytical method for evaluating the effects of adjacent excavation on shield tunnel considering the shearing effect”, *Comput. Geotech.*, **81**(2), 167-187.

Lu, A.Z., Xu, G.S., Sun, F. and Sun, W.Q. (2010), “Elasto-plastic analysis of a circular tunnel including the effects of the axial in situ stress”, *J. Rock. Mech. Min. Sci.*, **47**(1), 50-59.

Lukic, D.C., Prokic, A.D., Brcic, S.V., Lukic, D.C., Prokic, A.D. and Brcic, S.V. (2014). “Stress state around cylindrical cavities in transversally isotropic rock mass”, *Geomech. Eng.*, **6**(3), 213-233.

Mohamed, E.T. (2003), “Circular tunnel in a semi-infinite aquifer”, *Tunn. Undergr. Sp. Tech.*, **18**(1), 49-55.

Mohammadi, M. and Tavakoli, H. (2015), “Comparing the generalized hoek-brown and mohr-coulomb failure criteria for stress analysis on the rocks failure plane”, *Geomech. Eng.*, **9**(1), 115-124.

Pan, Q.J. and Dias, D. (2016), “The effect of pore water pressure on tunnel face stability”, *J. Numer. Anal. Met. Geomech.*, **40**(15), 2123-2136.

Pan, X.D. and Brown, E.T. (1996), “Influence of axial stress and dilatancy on rock tunnel stability”, *J. Geotech. Eng.*, **122**(2), 139-146.

Reed, M.B. (1988), “The influence of out-of-plane stress on a plane strain problem in rock mechanics”, *J. Numer. Anal. Met. Geomech.*, **12**(2), 173-181.

Sharan, S.K. (2008), “Analytical solutions for stresses and displacements around a circular opening in generalized Hoek-Brown rock”, *J. Rock Mech. Min. Sci.*, **45**(1), 78-85.

Shi, J.W., Wang, Y. and Ng, C.W.W. (2016), “Three-dimensional centrifuge modeling of ground and pipeline response to tunnel excavation”, *J. Geotech. Geoenviron.*, **142**(11), 0001529.

Shin, Y.J., Song, K.I., Lee, I.M. and Cho, G.C. (2011), “Interaction between tunnel supports and ground

convergence-Consideration of seepage forces", *J. Rock Mech. Min. Sci.*, **48**(3), 394-405.
Wan, L., Wei, Z. and Shen, J. (2016). Charts for estimating rock mass shear strength parameters", *Geomech. Eng.*, **10**(3), 257-267.
Wang, S.L., Wu, Z., Guo, M.W. and Ge, X.R. (2012a), "Theoretical solutions of a circular tunnel with the influence of axial in situ stress in elastic-brittle-plastic rock", *Tunn. Undergr. Sp. Tech.*, **30**(518-523), 155-168.
Wang, Y. (1996), "Ground response of circular tunnel in poorly consolidated rock", *J. Geotech. Eng.*, **122**(9), 703-708.
Yang, X.L. and Pan, Q.J. (2015), "Three dimensional seismic and static stability of rock slopes", *Geomech. Eng.*, **8**(1), 97-111.
Yang, X.L. and Yan, R.M. (2015), "Collapse mechanism for deep tunnel subjected to seepage force in layered soils", *Geomech. Eng.*, **8**(5), 741-756.
Yang, X.L. and Yin, J.H. (2010), "Slope equivalent Mohr-Coulomb strength parameters for rock masses satisfying the Hoek-Brown criterion", *Rock Mech. Rock Eng.*, **43**(4), 505-511.
Yang, X.L., and Qin, C.B. (2014). "Limit analysis of rectangular cavity subjected to seepage forces based on hoek-brown failure criterion", *Geomech. Eng.*, **6**(5), 503-515.
Yang, X.L., Xu, J.S., Li, Y.X. and Yan, R.M. (2016), "Collapse mechanism of tunnel roof considering joined influences of nonlinearity and non-associated flow rule", *Geomech. Eng.*, **10**(1), 21-35.
Yu, H. S. (2000), *Cavity Expansion Methods in Geomechanics*, Dordrecht: Kluwer Academic Publishers.
Zhang, L.M., Wu, X.G., Ji, W.Y. and AbouRizk, S.M. (2016). "Intelligent approach to estimation of tunnel-induced ground settlement using wavelet packet and support vector machines", *J. Comput. Civ. Eng.*, **30**(4), 0000621.
Zhou, H., Kong, G. and Liu, H. (2016), "A semi-analytical solution for cylindrical cavity expansion in elastic–perfectly plastic soil under biaxial in situ stress field", *Géotech.*, **66**(9), 1-3.
Zhou, H., Kong, G., Li, P. and Liu, H. (2015), "Flat cavity expansion: Theoretical model and application to the interpretation of the flat dilatometer test", *J. Eng. Mech.*, **212**(1), 1-7.
Zhou, H., Liu, H.L., Kong, G.Q. and Huang, X. (2014), "Analytical solution of undrained cylindrical cavity expansion in saturated soil under anisotropic initial stress", *Comput. Geotech.*, **55**(2), 232-239.
Zhou, X.P. and Li, J.L. (2011), "Hoek-Brown criterion applied to circular tunnel using elasto-plasticity and in situ axial stress", *Theor. Appl. Fract. Mec.*, **56**(2), 95-103.
Zhuang, L., Nakata, Y. and Lee, I.M. (2013). "Localized deformation in sands and glass beads subjected to plane strain compressions", *Geomech. Eng.*, **5**(6), 499-517.
Zou J.F. and Du J.M. (2017), "A new approach for the quasi-plane strain-softening problem of cylindrical cavity expansion based on Cam-Clay model", *J. Mech. Sci. Technol.*, **31**(3), 1315-1320.
Zou J.F., Du J.M. and Dan H.C. (2017d), "Solution for strain-softening surrounding rock reinforced by grouted bolts", *Adv. Mech. Eng.*, **9**(5), 1-18.
Zou, J.F. and Xia, M.Y. (2017a), "A new approach for the cylindrical cavity expansion problem incorporating deformation dependent of intermediate principal stress", *Geomech. Eng.*, **11**(3), 347-360.
Zou, J.F. and Xia, Z.Q. (2017b), "A closed-form solution for the cavity expansion in the strain-softening and undrained soil mass based on the unified strength failure criterion", *J. Geomech.*, **17**(9), 04017046.
Zou, J.F. and Zuo, S.Q. (2017), "Similarity solution for the synchronous grouting of shield tunnels under the non-axisymmetric displacement boundary on vertical surface", *Adv. Appl. Math. Mech.*, **9**(1), 205-232.
Zou, J. F., Li, C. and Wang, F. (2017c), "A new procedure for ground response curve (GRC) in strain-softening surrounding rock", *Comput. Geotech.*, **89**, 81-91.
Zou, J.F., Xia, Z.Q. and Dan, H.C. (2016), "Theoretical solutions for displacement and stress of a circular opening reinforced by grouted rockbolt", *Geomech. Eng.*, **11**(3), 439-455.

CC